STEM CELLS TRANSLATIONAL MEDICINE®

TISSUE-SPECIFIC PROGENITOR AND STEM CELLS

Safety of Epicenter Versus Intact Parenchyma as a Transplantation Site for Human Neural Stem Cells for Spinal Cord Injury Therapy

KATJA M. PILTTI,[a,b,c,d,*] DESIRÉE L. SALAZAR,[a,d,e,*] NOBUKO UCHIDA,[f] BRIAN J. CUMMINGS,[a,b,c,d] AILEEN J. ANDERSON[a,b,c,d]

Key Words. Spinal cord injury • Stem cell transplantation • Fate • Migration • CGRP • Mechanical allodynia • Thermal hyperalgesia

[a]Sue and Bill Gross Stem Cell Research Center, [b]Physical and Medical Rehabilitation, [c]Institute for Memory Impairments and Neurological Disorders, and [d]Anatomy and Neurobiology, University of California, Irvine, Irvine, California, USA; [e]Ludwig Institute for Cancer Research, University of California, San Diego, La Jolla, California, USA; [f]StemCells Inc., Newark, California, USA

[*]Contributed equally as first authors.

Correspondence: Aileen J. Anderson, Ph.D., 2030 Gross Hall Stem Cell Center, University of California Irvine, Irvine, California 92697, USA. Telephone: 949-824-6750; Fax: 949-824-9728; E-Mail: aja@uci.edu

Received September 4, 2012; accepted for publication December 5, 2012; first published online in SCTM *EXPRESS* February 14, 2013.

1066-5099/2013/$20.00/0

http://dx.doi.org/10.5966/sctm.2012-0110

ABSTRACT

Neural stem cell transplantation may have the potential to yield repair and recovery of function in central nervous system injury and disease, including spinal cord injury (SCI). Multiple pathological processes are initiated at the epicenter of a traumatic spinal cord injury; these are generally thought to make the epicenter a particularly hostile microenvironment. Conversely, the injury epicenter is an appealing potential site of therapeutic human central nervous system-derived neural stem cell (hCNS-SCns) transplantation because of both its surgical accessibility and the avoidance of spared spinal cord tissue. In this study, we compared hCNS-SCns transplantation into the SCI epicenter (EPI) versus intact rostral/caudal (R/C) parenchyma in contusion-injured athymic nude rats, and assessed the cell survival, differentiation, and migration. Regardless of transplantation site, hCNS-SCns survived and proliferated; however, the total number of hCNS-SCns quantified in the R/C transplant animals was twice that in the EPI animals, demonstrating increased overall engraftment. Migration and fate profile were unaffected by transplantation site. However, although transplantation site did not alter the proportion of human astrocytes, EPI transplantation shifted the localization of these cells and exhibited a correlation with calcitonin gene-related peptide fiber sprouting. Critically, no changes in mechanical allodynia or thermal hyperalgesia were observed. Taken together, these data suggest that the intact parenchyma may be a more favorable transplantation site than the injury epicenter in the subacute period post-SCI. STEM CELLS TRANSLATIONAL MEDICINE *2013;2:204–216*

INTRODUCTION

Human central nervous system-derived stem cells (hCNS-SCns) are one potential therapeutic cell population that has been tested for efficacy in several animal models of neurological disease and injury, including infantile neuronal ceroid lipofuscinosis (Batten's disease), Pelizaeus-Merzbacher disease, and traumatic spinal cord injury (SCI) [1–5]. hCNS-SCns are prospectively derived from 16–20-week-gestation fetal brain in combination with fluorescence-activated cell sorting for $CD133^{+}$ and $CD24^{-/lo}$ cell surface markers [6].

Traumatic SCI results in partial or complete paralysis along with sensory loss below the level of injury. SCI pathology is characterized by loss of neurons and oligodendrocytes, axonal injury, and demyelination and dysmyelination of spared axons. We have previously shown that transplantation of hCNS-SCns into the intact parenchyma rostral and caudal to the SCI epicenter, either subacutely [2, 3] or in the early chronic stage postinjury [1], improved locomotor recovery after SCI. In that paradigm, hCNS-SCns showed robust engraftment and differentiation into all three neural lineages, with a majority of cells exhibiting an oligodendrocyte fate 16 weeks post-transplant (wpt) [1–3]. hCNS-SCns also exhibited remyelination of host axons and synapse formation with host neuronal circuitry; however, no evidence of host regeneration or other modulation of the host microenvironment was detected [2, 3]. We have also demonstrated that selective ablation of hCNS-SCns-derived cells from NOD-scid mouse spinal cord using diphtheria toxin resulted in a loss of locomotor improvement, suggesting hCNS-SCns integration/host cell replacement as a mechanism for recovery [2].

Critically, after SCI, humans and rats form a fluid-filled cystic cavity, whereas mice form a fibrotic matrix at the injury epicenter. In either case, a glial scar develops around the epicenter, restoring blood-brain barrier integrity and restricting inflammatory cell infiltration [7–9] but generating a physical and molecular barrier to regeneration [10, 11]. Multiple pathological processes are initiated at the SCI epicenter, and these are often thought to make this site a particularly hostile microenvironment for cell transplantation [12–14]. Conversely, the injury

epicenter is an appealing potential site of therapeutic cell transplantation because it is surgical accessible and injections into the epicenter avoid spared spinal cord tissue.

Accordingly, fibroblasts, Schwann cells, olfactory ensheathing glia, mesenchymal cells, embryonic stem cell-derived neuronal and oligodendroglial progenitors, and neural stem cells have all been transplanted into this region for experimental evaluation [13, 15–24]; however, few publications have directly compared epicenter and parenchymal transplantation. Additionally, studies testing multipotent neural stem cell (NSC) transplantation into the SCI epicenter have been performed in either immunocompetent or immunosuppressed SCI models [16, 20, 22, 24]. Critically, the use of immunocompetent models, especially for discordant xenografts, is problematic because these models do not support reliable donor cell engraftment, negatively affecting their predictive validity [25]. Furthermore, several of these studies used multilevel laminectomies (which can significantly destabilize the spinal column), immortalized cells, or concomitant local trophic factor administration, and only one has directly compared epicenter versus rostral/caudal transplantation with rodent NSCs [22]. In the latter study, no immunosuppression was administered, and the data for animals receiving parenchymal versus epicenter transplantation were not reported separately. Although transplanted cells in these studies did exhibit at least short term engraftment, cell fate was predominantly astroglial, with few engrafted cells exhibiting neural or oligodendrocytic lineage-specific differentiation markers [20, 22, 24]. Critically, predominant astroglial cell fate after transplantation of rodent NSCs has been shown to correlate with allodynia, a chronic pain syndrome frequently suffered by individuals with SCI [23, 24, 26, 27]. If the site of transplantation directs astroglial fate, or induces allodynia, this would have significant influence on the design of future clinical trials.

T cells have been shown to contribute to development of neuropathic pain, but they are also the major player in acute rejection of transplanted cells and organs [25, 28]. Stable allogeneic or xenogeneic transplantation of stem cells requires either suppression of T cells via administration of pharmacological immunosuppressants (e.g., cyclosporine), or the use of constitutively immunodeficient animal models such as the athymic nude (ATN) rat or NOD-scid mouse [25, 28]. Critically, although ATN rats lack mature T cells, previous studies have shown that these animals can be used as a neurological pain syndrome model [29].

Accordingly, we investigated the effect of transplantation site on hCNS-SCns survival, engraftment, migration and fate, lesion and spared tissue volume, and development of anatomical or behavioral evidence of allodynia/hyperalgesia. Together, the data suggest that transplantation into the intact parenchyma rostral/caudal to the injury epicenter may be a more favorable transplantation site than the injury epicenter in the subacute period post-SCI.

Materials and Methods

Animal Welfare

This study was carried out in accordance with the Institutional Animal Care and Use Committee at the University of California, Irvine, and in consistency with U.S. federal guidelines.

Contusion Injuries

Adult female 10–11-week-old, 180–200-g ATN rats (National Cancer Institute, Frederick, MD, http://frederick.cancer.gov) were anesthetized with 2.5% isoflurane and maintained under 3% isoflurane (VetEquip Inc., Pleasanton, CA, http://www.vetequip.com) during the surgery. Spinal cords at thoracic 9 (T9) vertebral level were exposed by laminectomy using a surgical microscope and stabilized in a spinal stereotaxic frame by clamping at the T8 and T10 lateral vertebral processes, and bilateral 200-kDa contusion injuries were administrated using an Infinite Horizon Impactor (Precision Systems and Instrumentation, Lexington, KY, http://www.presysin.com). Following the injury, the exposed spinal cords were covered with gelfoam (Pfizer, New York, NY, http://www.pfizer.com), muscles were reattached with 5-0 chromic gut sutures (Surgical Specialties Co., Reading, PA, http://www.heidolphna.com), and the skin was closed using wound clips (CellPoint Scientific Inc., Gaithersburg, MD, http://www.cellpointscientific.com). For postoperative care, the animals received subcutaneous injections of 0.01 mg/kg buprenorphine (Hospira Inc., Lake Forest, IL, http://www.hospira.com) twice a day for 2 days, 50 ml/kg lactated Ringer's solution (B. Braun Medical Inc., Irvine, CA, http://www.bbraunusa.com) once daily for 4 days, and bladder expression twice daily for 1 month postinjury and then once daily until the end of study. All the animals were maintained on oral antibiotics by rotating 800 μg/ml sulfamethoxalone-trimethoprim (Hi-Tech Pharmacal, Amityville, NY, http://www.hitechpharm.com), 200 μg/ml ampicillin (STADA Pharmaceuticals, Cranbury, NJ, http://www.stada.de/english), and 100 μg/ml ciprofloxacin hydrochloride (Dr. Reddy's Laboratories, Bachepalli, India, http://www.drreddys.com) in drinking water every third week until end of the study.

hCNS-SCns Transplantation

hCNS-SCns (StemCells Inc., Palo Alto, CA, http://www.stemcellsinc.com) were cultured as neurospheres in supplemented X-Vivo 15 medium (Lonza, Basel, Switzerland, http://www.lonza.com) as previously described [6]. Prior to transplantation, neurospheres at passage number 12 or less were dissociated into individual cells and adjusted into cell density of 50,000 cells per microliter in X-Vivo 15 medium (Lonza). Rats were reanesthetized 9 days postinjury (dpi), the laminectomy sites were re-exposed, and the cords were stabilized in a spinal stereotaxic frame. For hCNS-SCns transplantation rostral/caudal (R/C) location to the injury epicenter, a total volume of 4 μl (1 μl per injection site) of cell suspension or vehicle (X-Vivo 15 medium) was injected in two rostral bilateral injections through the intervertebral cartilage space at T7/T8 and another two caudal injections through the intervertebral cartilage space at T10/T11 using polished 30° beveled glass pipettes (inner diameter [i.d.] = 75–80 μm, outer diameter [o.d.] = 100–115 μm) (Sutter Instrument, Novato, CA, http://www.sutter.com), a NanoInjector 2000 system (World Precision Instruments, Waltham, MA, http://www.wpiinc.com), and a micropositioner (World Precision Instruments) under microscopic guidance. For hCNS-SCns transplantation in spinal cord injury epicenter (EPI), a total volume of 4 μl of cell suspension or vehicle was injected directly into the bruised spinal cord tissue at T9 using a NanoFil syringe with a 33-gauge Flexifil tip (200 μm o.d., 100 μm i.d.) (World Precision Instruments) over 5 minutes, followed by an additional 5-minute

delay before removing the needle to prevent backflow. After transplantation, the postoperative procedures were performed as described above.

Randomization, Exclusion Criteria, and Group Numbers

Randomization, exclusion criteria, and blinding for assessments were conducted as described previously [1–3]. Prior to transplantation, rats were randomized across cohorts, and equivalent behavioral baselines confirmed for each cohort using open-field Basso, Beattie, and Bresnahan (BBB) locomotor scores 7 dpi. Animals with unilateral bruising or abnormal force/displacement curves after contusion injury, or in which a vertebral T9 laminectomy could not be confirmed at the time of cell transplantation, were excluded from sensory behavioral and stereological assessments. All cohorts were conducted in parallel; that is, animals received spinal cord injuries at the same age and during the same week of surgery. All animal care, behavioral assessments, and histological processing/analysis were performed by observers blinded to experimental cohort. hCNS-SCns engraftment was confirmed in all animals, and a subset of spinal cords from animals in all cohorts was randomly selected for stereological analysis. SC121 immunostaining revealed that two of nine rats selected from the R/C hCNS-SCns cohort showed very poor or no engraftment; these rats were excluded from further sensory behavioral and stereological analysis and from statistical analysis other than reporting of the percentage of engrafted animals. Final cohort numbers (n) for sensory assessment were therefore as follows: hCNS-SCns R/C, $n = 10$; vehicle R/C, $n = 12$; hCNS-SCns EPI, $n = 12$; vehicle EPI, $n = 12$. Final cohort numbers for histology/stereology were therefore as follows: hCNS-SCns R/C, $n = 7$; vehicle R/C, $n = 8$; hCNS-SCns EPI, $n = 7$; vehicle EPI, $n = 8$ (supplemental online Table 1).

Sensory Behavior Assessments

For mechanical allodynia assessment using von Frey testing [30], rats were placed in a clear acrylic chamber on an elevated wire mesh grid. Withdrawal response of all four paws was assessed by applying 1.4 gram low force and 6.0 gram high force Touch-Test Sensory Evaluator filaments (North Coast Medical, Gilroy, CA, https://www.ncmedical.com) prior to injury (baseline) and at 2, 7, 11, and 14 wpt. Filaments were administered to the plantar surface of each paw 10 times, 2 minutes apart, and the number of withdrawals was recorded.

For thermal hyperalgesia assessment using Hargreaves testing [30–32], rats were placed in an elevated Plexiglas chamber on top of a temperature-controlled glass plate heated to 30°C. A withdrawal response of all four paws was assessed using a radiant thermal stimulus of the paw analgesia meter set at an active intensity of 35 (arbitrary units) applied to the plantar surface through the glass plate (IITC Life Sciences, Inc, Woodland Hills, CA, http://www.iitcinc.com) prior to injury (baseline) and at 2, 7, 11, and 14 wpt. Thermal stimulus was administered to plantar surface of each paw three times, 3 minutes apart, and the reaction times were recorded and then averaged.

For both von Frey and Hargreaves, animals were acclimatized to the testing chambers for 1 h prior to testing.

Perfusion and Tissue Collection

At 14 wpt, rats were injected with a lethal dose of Euthasol (Virbac AH, Fort Worth, TX, http://www.virbacvet.com) and transcardially perfused with phosphate buffered saline followed by 4% paraformaldehyde (PFA) (Fisher Scientific, Fairlawn, NJ, http://www.fishersci.com). Spinal cord T6–T12 vertebral regions were dissected based on dorsal spinal root counts, post-fixed overnight in 4% PFA supplemented with 20% sucrose, flash frozen at −65°C in isopentane (Fisher Scientific), and stored for sectioning at −80°C.

Tissue Sectioning and Immunohistochemistry

For 3,3′-diaminobenzidine (DAB) peroxidase immunohistochemistry, whole T6–T12 spinal cord segments were cut into 30-μm-thick coronal sections using a cryostat (ThermoScientific, Barrington, IL, http://www.thermoscientific.com) and transferred onto slides using a CryoJane tape transfer system (Leica Microsystems Inc., Buffalo Grove, IL, http://www.leica-microsystems.com). Tissue sections on slides in a sequence of 1/24 underwent antigen retrieval in R-buffer A (Electron Microscopy Sciences, Hatfield, PA, http://www.emsdiasum.com/microscopy) using a 2100 Retriever (PickCell Laboratories, Amsterdam, The Netherlands, http://www.amsterdambiomed.nl), treated with a solution of Tris (0.1 M Tris, pH 7.4), 3% hydrogen peroxide (Fisher Scientific), and 10% methanol (Fisher Scientific) for 20 minutes to deactivate endogenous peroxide activity. Immunocytochemistry was conducted as previously described [3]. For fluorescence-conjugated immunohistochemistry, whole T6–T12 spinal cord segments were embedded, and cut into 30-μm-thick coronal sections using a HM 450 MicroM microtome (ThermoScientific). Sections in a sequence of 1/24 were permeabilized, exposed to primary antibodies followed by exposure to DyLight fluorescence-conjugated affinipure $F(ab')_2$ fragment secondary antibodies (Jackson Immunoresearch Laboratories, West Grove, PA, http://www.jacksonimmuno.com) before mounting onto slides. Hoechst 33342 (Invitrogen, Grand Island, NY, http://www.invitrogen.com) was used for nuclear labeling. A z-stack of optical sections was acquired using an ApoTome system on a Zeiss AxioImager M2 microscope (Carl Zeiss, Maple Grove, MN, http://www.zeiss.com).

The primary antibodies used were directed against human cytoplasm SC121 (STEM121; Stem Cell Science, Cambridge, U.K., http://www.stemcellsciences.com), human glial fibrillary acidic protein SC123 (STEM123; Stem Cell Science), pan-glial fibrillary acidic protein (GFAP) (BD Pharmingen, San Diego, CA, http://www.bdbiosciences.com), doublecortin (DCX; Santa Cruz Biotechnology Inc., Santa Cruz, CA, http://www.scbt.com), β-tubulin III (Covance, San Diego, CA, http://www.covance.com), Olig2 (R&D Systems Inc., Minneapolis, MN, http://www.rndsystems.com), and calcitonin gene-related peptide (CGRP; Sigma-Aldrich, St. Louis, MO, http://www.sigmaaldrich.com).

Stereological Quantification

Final numbers for analysis are as described above and listed in supplemental online Table 1. Total numbers of $SC121^+$ human cells and $SC123^+$ human astrocytes were determined by unbiased stereology in 1/24 intervals from spinal cord sections 0.72 mm apart using systematic random sampling with an optical fractionator probe and StereoInvestigator version 9 (MicroBrightField Inc., Williston, VT, http://www.mbfbioscience.com). Optical fractionator grid size and counting frame size were empirically determined to yield average cumulative error values less than 0.1 (supplemental online Table 2). The number of $SC121^+$/$Olig2^+$ and $SC121^+$/DCX^+ cells were analyzed in 1/48 intervals

from spinal cord sections 1.44 mm apart using an optical fractionator probe and systematic random sampling according to stereological principles (supplemental online Table 2).

A Cavalieri probe (SI9; MicroBrightField) was used to analyze total volumes of spinal cord, lesion, and dorsal horn CGRP fibers in 1/24 intervals from coronal spinal cord sections 0.72 mm apart at ×4 magnification (supplemental online Table 2). As a tape transfer system was used to preserve tissue integrity, lesion volume was quantified as the area lacking any spinal cord tissue (e.g., the lesion cavity). A spaceball probe with a 12-μm hemisphere was used to analyze CGRP fiber length in dorsal horn laminae III and IV rostral to lesion cavity in 1/24 intervals from coronal spinal cord sections 0.72 mm apart. A contour was drawn around laminae III and IV at ×60 magnification, identified by the pattern of nuclear staining, and the fiber length was assessed at ×100 magnification (supplemental online Table 2).

Migration of SC121$^+$ or SC123$^+$ human cells was analyzed as percentage of the cells per section relative to total number of counted SC121$^+$ human cells. To compare cell migration between the hCNS-SCns transplantation cohorts, the distribution of the cells was normalized with the distance from the injection site, in the R/C cohort designated as section with highest percentage of the SC121$^+$ cells relative to total number of the human cells and in the EPI cohort designated as the most damaged tissue section with largest cavity.

Statistical Analysis

All data are shown as mean ± SEM; statistical analysis were performed using Prism4 software (GraphPad Software, Inc., San Diego, CA, http://www.graphpad.com). Von Frey and Hargreaves scores were compared using two-way repeated-measures analysis of variance (ANOVA) combined with Bonferroni post hoc *t* tests. Correlation between CGRP length or volume, and numbers of SC123$^+$ or SC121$^+$ cells, and Hargreaves or von Frey measures were assessed using Pearson correlation coefficient. Comparisons between cohorts were analyzed using either one-way ANOVA combined with Tukey's post hoc *t* test or Student's two-tailed *t* test. A p value $\leq .05$ was considered to be statistically significant.

RESULTS

hCNS-SCns Exhibited Greater Survival and Migration in R/C Versus EPI Transplant Animals

To assess effect of transplantation site on hCNS-SCns survival at 14 wpt, we conducted immunohistochemistry for the human-specific cytoplasmic marker SC121. Vehicle-treated animals exhibited no positive staining for SC121 (Fig. 1A, 1B). Cohort numbers for analysis were as described in Materials and Methods and in supplemental online Table 1. Animals exhibiting either caudal-only engraftment (presumed to be injection failure) or no detectable human cells were excluded from further analysis (as described in Materials and Methods and indicated in red in Fig. 1C). Based on these exclusion criteria, spinal cords analyzed from both transplantation cohorts showed good engraftment: 88.9% of R/C hCNS-SCns animals and 100% of EPI hCNS-SCns animals exhibited extensive numbers of SC121$^+$ cells at 14 wpt. No animals in either cohort exhibited any evidence of mass formation or abnormal morphology by human cells that would suggest tumorigenesis.

Stereological quantification revealed that the total average estimated number of SC121$^+$ human cells was 1,114,000 ± 94,780 (557 ± 47% of the initial transplant dose) in the R/C hCNS-SCns cohort and 498,100 ± 70,140 (249 ± 35% of the initial transplant dose) in the EPI hCNS-SCns cohort (Fig. 1C). These values reflect a significant increase in engrafted cells in the R/C in comparison with the EPI transplant cohort (Student's two-tailed *t* test; ***, $p < .0002$), demonstrating that R/C transplantation of hCNS-SCns at 9 dpi increased cell engraftment as a result of altered survival and/or proliferation.

In addition to these differences in engraftment, significant differences in hCNS-SCns localization were also observed between the R/C and EPI transplanted animals. For this assessment, sections were aligned by location relative to the injury epicenter, designated as the most damaged tissue section with largest scar. In the R/C cohort, the majority of hCNS-SCns were localized in white matter in the distal spinal cord and rarely found near the injury epicenter (Figs. 1D, 2A; supplemental online Movie 1). In contrast, hCNS-SCns in the EPI cohort were most frequently located in spared tissue adjacent to the injury epicenter. The percentage of SC121$^+$ human cells per section was significantly greater in the distal parenchyma in R/C compared with EPI transplant animals, and the EPI hCNS-SCns cohort showed a significantly higher proportion of human cells near the injury epicenter (Fig. 1D, Student's two-tailed *t* test; *, $p < .05$; **, $p < .007$). Regardless of transplantation site, hCNS-SCns were rarely found in the cystic cavity at 14 wpt (Figs. 1D, 2A; supplemental online Movie 2).

At first glance, the cell distribution in Figure 1D suggests that the EPI transplant site may limit hCNS-SCns migration capacity. However, it is also possible that these apparent differences reflect the initial transplantation site, in which case both EPI and R/C hCNS-SCns cohorts would be predicted to show equivalent migration distance. Accordingly, the farthest point of human cell migration relative to the injury epicenter was analyzed to determine the migration range. The R/C hCNS-SCns cohort exhibited a migration range of 14.4 mm rostral and 14.4 mm caudal from the injury epicenter, with a total spread of 28.8 mm (Figs. 1D, 2A). The EPI hCNS-SCns cohort exhibited a migration range of 11.5 mm rostral and 14.4 mm caudal from the injury, with a total spread of 25.9 mm (Figs. 1D, 2A). We further investigated the effect of transplantation site on hCNS-SCns migration by normalizing the number of human cells quantified in the EPI and R/C transplant cohorts relative to the location of the initial injection site. This analysis revealed no significant differences between the cohorts (Fig. 1E, Student's two-tailed *t* test, $p > .05$). Taken together, these data suggest that transplantation site does not affect hCNS-SCns migration capacity in the subacute SCI environment.

We have not previously observed changes in lesion or spared tissue volume in immunodeficient mice after hCNS-SCns transplantation in intact rostral and caudal parenchyma at the subacute or early chronic stages of spinal cord injury [3, 33]. To determine whether hCNS-SCns transplantation site altered lesion or spared tissue volume in the present study, tissue sections were analyzed using unbiased stereology. No significant differences in spared tissue or lesion volume were found between any of the cell or vehicle control cohorts (Fig. 2B, 2C; one-way ANOVA, $p < .05$), suggesting that the transplantation site with this hCNS-SCns dose and at this stage of injury did not affect lesion or spared tissue volume.

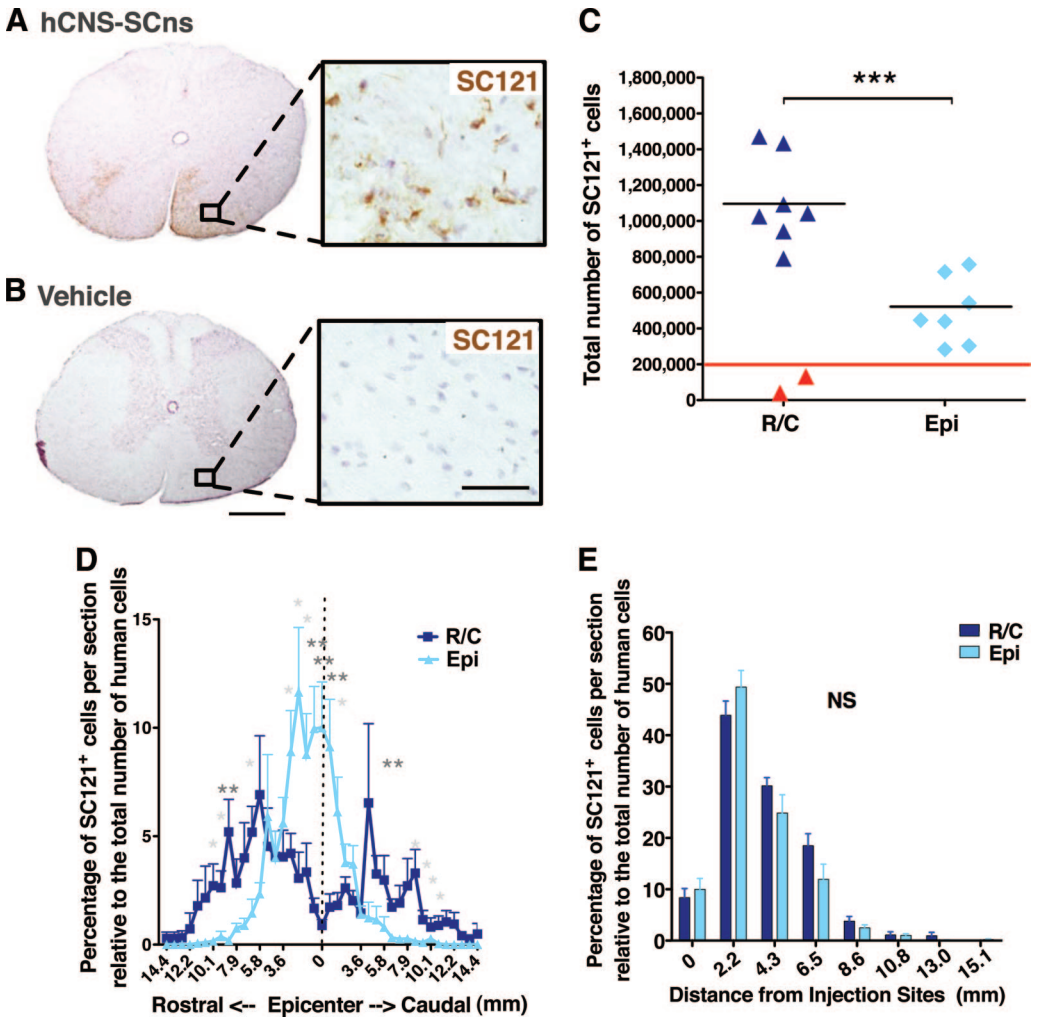

Figure 1. hCNS-SCns engraft, survive, and migrate in both transplantation sites. **(A, B):** Transplanted, engrafted spinal cords showed human-specific cytoplasmic marker SC121$^+$ cells **(A)**, unlike the vehicle-treated cords **(B)** at 14 weeks post-transplant. Scale bars = 500 and 50 μm. **(C):** Unbiased analysis using the StereoInvestigator optical fractionator revealed that the total estimated numbers of SC121$^+$ cells were significantly higher in R/C cohort compared with those in the Epi cohort (Student's two-tailed *t* test; ***, $p < .0002$). Red line indicates the initial transplantation dose; red triangles indicate the animals excluded because of bad engraftment. **(D):** Cell migration shown as percentage of SC121$^+$ cells per section relative to total number of counted human cells (Student's two-tailed *t* test; *, $p < .05$; **, $p < .007$). **(E):** Migration of SC121$^+$ cells normalized by distance from the injection sites (Student's two-tailed *t* test; $p > .05$). Error bars indicate SEM. Abbreviations: Epi, epicenter; hCNS-SCns, human central nervous system-derived neural stem cell; NS, not significant; R/C, rostral/caudal.

Transplantation Site Did Not Affect hCNS-SCns Cell Fate in the ATN Rat SCI Model

We have previously reported that in immunodeficient mice, the majority of multipotent hCNS-SCns differentiate into oligodendrocyte lineage cells after transplantation into the intact spinal cord parenchyma either subacutely 9 days or at early chronic stage 30 days post-contusion injury [1–3]. In contrast, transplantation of rodent neural stem cells after contusion SCI in immunosuppressed or immunocompetent rats has in some cases been reported to result in astrogliogenesis or retention of undifferentiated cells [22, 24]. To study the effect of transplantation site on neural stem cell differentiation in immunodeficient ATN rats, we quantified the percentages of human cells positive for the oligodendroglial lineage marker nuclear Olig2, the immature neuronal marker DCX, or the human-specific astrocyte marker SC123 (human GFAP).

Quantification revealed that the average proportion of SC121$^+$/Olig2$^+$ cells (Fig. 3A) in R/C hCNS-SCns spinal cords was 52.0 $\pm$ 3.2% and in EPI hCNS-SCns spinal cords was 44.3 $\pm$ 4.9%; no significant difference between these cohorts was found (Fig. 3B, Student's two-tailed *t* test). Confocal imaging of immunohistochemical staining for Olig2/SC123, or Olig2/SC121/β-tubulin III, showed that nuclear Olig2 did not overlap with either human origin astrocytes or neurons and was most consistent with early oligodendrocyte lineage cells (supplemental online Figs. 1, 2). However, as previously reported, we did find coexpression of nuclear Olig2 and the mature oligodendrocyte marker APC/CC-1 in human cells at 14 wpt (supplemental online Fig. 3). In parallel, quantification of human neuronal lineage cells revealed that the proportion of SC121$^+$/DCX$^+$ cells (Fig. 3C) in the R/C hCNS-SCns spinal cords was 6.1 $\pm$ 0.5%, and in the EPI hCNS-SCns spinal cords was 9.0 $\pm$ 1.5%; again, no significant differences between these cohorts was found (Fig. 3D, Student's two-tailed *t* test, $p > .05$). A small proportion of human SC121$^+$/DCX$^+$ cells were also positive for the more mature neuronal marker β-tubulin III (supplemental online Fig. 4). Finally, quantification of human

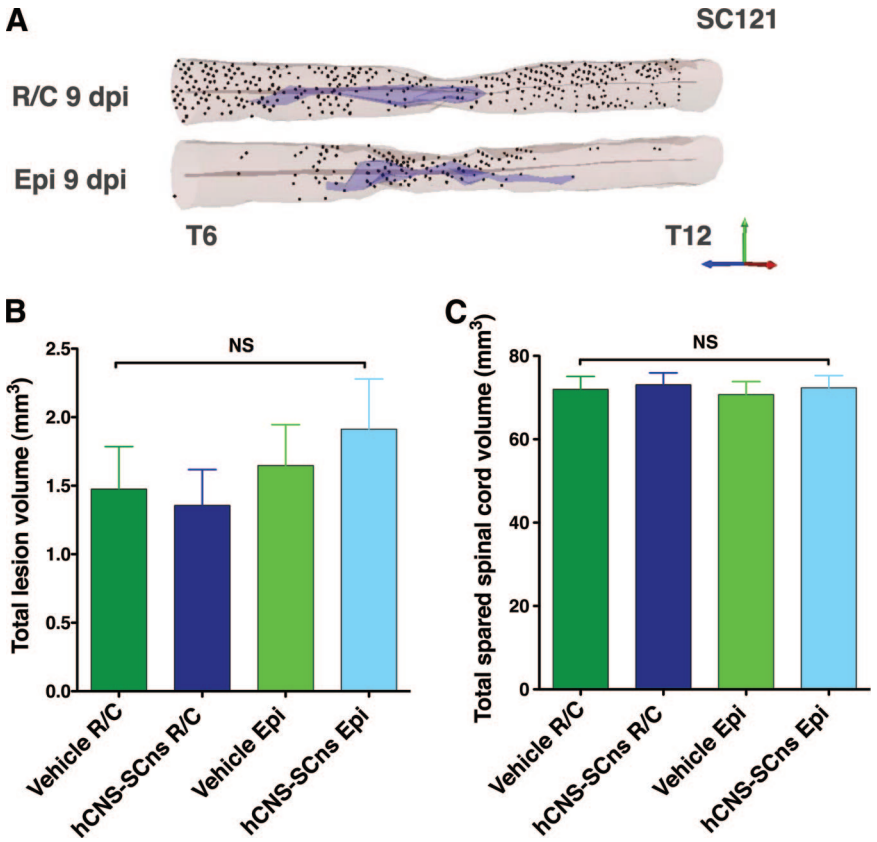

Figure 2. Distribution of hCNS-SCns differs, but the cells do not alter lesion or spared tissue volume when transplanted either in intact parenchyma or injury epicenter. **(A):** Three-dimensional reconstruction of the spinal cords transplanted at R/C and Epi sites showing location of analyzed SC121$^+$ human cells based on StereoInvestigator optical fractionator probe quantification data analyzed from coronal sections in 1/24 sampling sequence at 14 weeks post-transplant. Shown are human cells (dots), central canal (gray lines), and injury cavity (purple). The StereoInvestigator Cavalieri probe did not reveal changes in spared spinal cord tissue **(B)** or lesion volumes **(C)** between the cohorts (one-way analysis of variance; $p > .05$). Error bars indicate SEM. Abbreviations: Epi, epicenter; hCNS-SCns, human central nervous system-derived neural stem cell; NS, not significant; R/C, rostral/caudal.

astrocytic lineage cells revealed that the proportion of SC123$^+$ cells (Fig. 4A) was 41 $\pm$ 4.1% in the R/C hCNS-SCns spinal cords, compared with 42 $\pm$ 6.3% in the EPI hCNS-SCns spinal cords; again, no statistically significant difference was observed between these cohorts (Fig. 4B, Student's two-tailed *t* test, $p >$ .05). Taken together, these data show that 99.1% of hCNS-SCns in the R/C cohort and 94.8% of hCNS-SCns in the EPI cohort were positive for either nuclear Olig2, DCX, or SC123 at 14 wpt. These data suggest that a majority of hCNS-SCns exhibited neural lineage differentiation, with robust expression of oligodendroglial markers when transplanted into immunodeficient SCI rats. Moreover, the location of transplantation did not alter the fate of engrafted hCNS-SCns when transplanted at 9 dpi.

Interestingly, the proportion of human astrocyte lineage cells observed in the present study in SCI ATN rats was higher than we have previously found after hCNS-SCns transplantation into SCI NOD-scid mice [1–3]. Investigation of the localization of SC123$^+$ cells revealed that in the R/C transplant cohort, human astrocytes were found up to 14.4 mm rostral and 7.9 mm caudal from the injury epicenter, with a total spread of 22.3 mm (Fig. 4C, 4E). In the EPI transplant cohort, human astrocytes were found up to 12.2 mm rostral and 2.9 mm caudal from the injury epicenter, with a total spread of 15.1 mm (Fig. 4C, 4E). In the R/C transplant cohort, the percentage of SC123$^+$ cells per section expressed as a proportion of the total number of human cells was highest in the rostral parenchyma but exhibited an even distribution (Fig. 4C, 4E; supplemental online Movies 3, 4). In contrast, in the EPI transplant cohort the majority of SC123$^+$ human astrocytes were strikingly localized to the rostral parenchyma adjacent to the injury epicenter designated based on identification of the tissue section containing the largest cross-sectional lesion area (Fig. 4C, Student's two-tailed *t* test; $*$, $p < .05$; $**$, $p < .01$; $***$, $p < .001$). However, a majority of ATN rats exhibited large cavities extending into the rostral spinal cord, as observed in the three-dimensional reconstruction examples (Fig. 3E). When the distribution of human SC123$^+$ astrocytes in both transplant cohorts was normalized relative to the initial injection site, a greater proportion of SC123$^+$ cells in the EPI cohort was found further away from the injection site compared with those in the R/C cohort (Fig. 4D, Student's two-tailed *t* test; $*$, $p < .05$; $**$, $p < .005$; $***$, $p < .001$). These data suggest that even though the transplantation site did not alter the overall proportion of hCNS-SCns exhibiting astroglial differentiation, the localization of these cells within the injured spinal cord was altered.

Effect of Transplantation Site on CGRP Fiber Sprouting and Behavioral Measures of Allodynia/Hyperalgesia

Disruption of the sensory nerve tracks of SCI subjects can lead to chronic pain syndromes, such as allodynia and hyperalgesia. Allodynia is increased sensitivity to a stimulus that is not normally

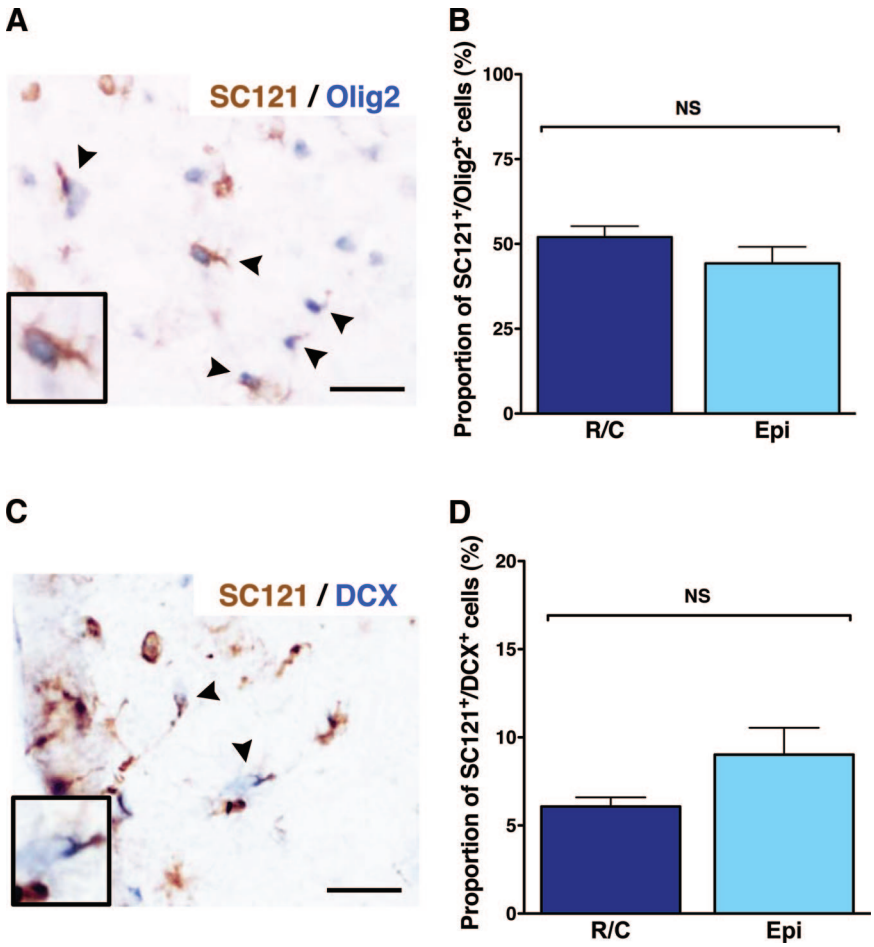

Figure 3. Human central nervous system-derived neural stem cell (hCNS-SCns) transplantation site does not affect differentiation into oligodendroglial or neural cell lineages. The majority of hCNS-SCns in both cohorts differentiated into $SC121^+/Olig2^+$ human oligodendroglial cells (arrowheads) at 14 weeks post-transplant **(A)**, and no significant difference was found between the cohorts **(B)** (Student's two-tailed *t* test; $p > .05$). A small proportion of hCNS-SCns in both cohorts differentiated into $SC121^+/DCX^+$ human immature neurons (arrowheads) **(C)**, and no significant difference was found between the cohorts **(D)** (Student's two-tailed *t* test; $p > .05$). Scale bars = 25 μm. Error bars indicate SEM. Abbreviations: DCX, doublecortin; Epi, epicenter; NS, not significant; R/C, rostral/caudal.

noxious. Hyperalgesia is increased sensitivity to a noxious stimulus [27, 34]. Initiation of a chronic pain syndrome as the result of a therapeutic intervention would be a significant adverse event. Both transplantation site and astroglial fate could potentially alter the volume and length of CGRP sensory fibers, which are involved in transmission and modulation of pain and sensory information [35, 36]. Accordingly, we measured CGRP sensory fiber sprouting in dorsal horn laminae III–IV by two methods, determination of fiber volume and length (Fig. 5A), in all four cohorts of SCI rats: R/C vehicle, R/C hCNS-SCns, EPI vehicle, and EPI hCNS-SCns.

Quantification of CGRP volume and fiber length revealed no significant differences in any of the cohorts (Fig. 5B, 5C, Student's *t* test, $p > .1$). Furthermore, no relationship was observed between (a) CGRP fiber volume and the total number of $SC121^+$ cells in the EPI or R/C transplant cohorts (Pearson $r = 0.3$, $p > .5$, and $r = 0.2$, $p > .6$, respectively); (b) CGRP fiber volume and the total number of $SC123^+$ human astrocytes in the EPI or R/C transplant cohorts (Pearson $r = -0.3$, $p > .5$, and $r = 0.5$, $p > .2$, respectively); or (c) CGRP fiber length and the total number of $SC121^+$ human cells or $SC123^+$ astrocytes in the R/C transplant cohort (Fig. 5D, 5E, Pearson $r = -0.04$, $p > .9$, and $r = -0.6$, $p > .1$, respectively). However, in the EPI transplant cohort, a significant positive correlation was found between CGRP fiber length and the total number of $SC121^+$ human cells (Fig. 5F, Pearson $r = 0.83$; $*$, $p < .02$) as well as the total number of $SC123^+$ human astrocytes (Fig. 5G, Pearson $r = 8.7$; $*$, $p < .01$). These data suggest no evidence for altered CGRP volume or sprouting in association with R/C hCNS-SCns transplantation. However, despite the lower number of total engrafted human cells, EPI hCNS-SCns transplantation may be associated with increased CGRP fiber sprouting.

To investigate whether hCNS-SCns transplantation site or fate induced changes in behavioral measures of mechanical allodynia or thermal hyperalgesia, we assessed these parameters in all cohorts prior to injury and 2, 7, 11, and 14 wpt. No significant two-way interaction effects were observed between hCNS-SCns versus vehicle groups over time in the number of forepaw or hind paw withdrawals in any of the cohorts using either a low (data not shown) or a high force filament in von Frey testing (Fig. 6A–6D; repeated-measures two-way ANOVA, Bonferroni post hoc test, $p > .05$). Similarly, no significant two-way interaction effects in forepaw or hind paw withdrawal time were found in Hargreaves testing (Fig. 6E–6H; repeated-measures two-way

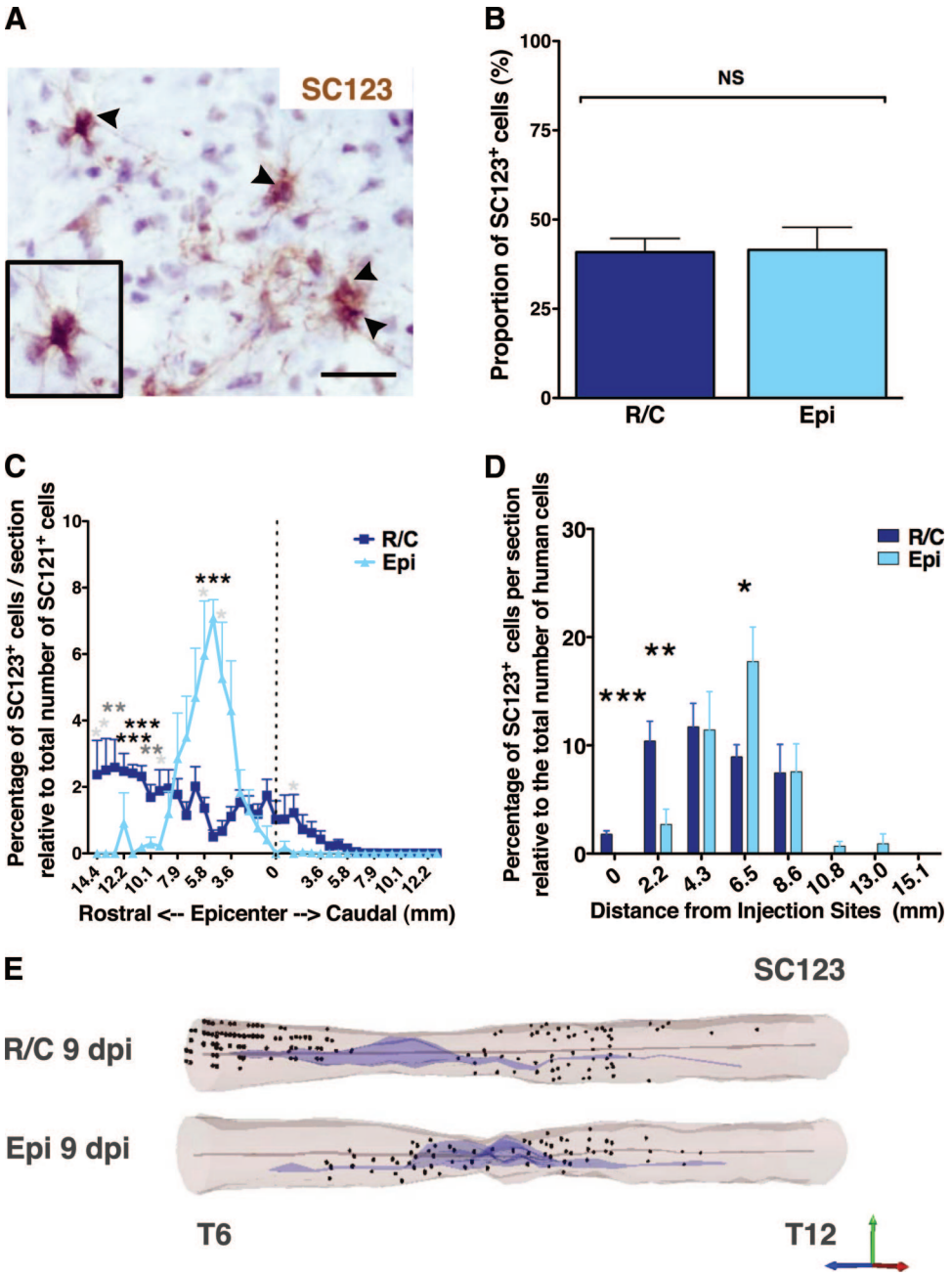

Figure 4. Transplantation site does not affect the proportion but does affect the localization of human astrocytes. Immunohistochemistry with human-specific glial fibrillary acidic protein antibody SC123 (arrowheads) **(A)** revealed that the transplantation site did not affect human central nervous system-derived neural stem cell (hCNS-SCns) differentiation into astroglial cell lineage **(B)**. Athymic nude (ATN) rats showed a relatively high proportion of $SC123^+$ human astrocyte lineage cells **(A)**, but no significant difference was found between the cohorts **(B)**; Student's two-tailed *t* test; $p > .05$. Scale bar = 25 μm. **(C):** Human astrocyte migration shown as percentage of $SC123^+$ cells per section relative to total number of counted $SC121^+$ human cells (Student's two-tailed *t* test; *, $p < .05$; **, $p < .01$; ***, $p < .001$). Error bars indicate SEM. Positional data are plotted relative to the injury epicenter (dashed vertical line), which was designated on the basis of identification of the tissue section containing the largest cross-sectional lesion area; however, a majority of ATN rats exhibited large cavities extending into the rostral spinal cord as observed in the three-dimensional (3D) reconstruction examples in **(E)**. **(D):** Migration of $SC123^+$ astrocytes normalized by distance from the injection (Student's two-tailed *t* test; *, $p < .05$; **, $p < .005$; ***, $p < .001$). **(E):** 3D reconstruction of the spinal cords transplanted at R/C and Epi sites showing location of analyzed $SC123^+$ human astrocytes based on StereoInvestigator optical fractionator probe quantification data analyzed from coronal sections in 1/24 sampling sequence at 14 weeks post-transplant. Shown are human astrocytes (dots), central canal (gray lines), and injury cavity (purple). Abbreviations: dpi, days postinjury; Epi, epicenter; NS, not significant; R/C, rostral/caudal.

ANOVA, Bonferroni post hoc *t* test, $p > .05$). In addition, no significant correlation was found between (a) the total number of $SC121^+$ human cells and the allodynia (statistical values are given in supplemental online Table 3) or hyperalgesia measures (Fig. 7A, 7B, Pearson $r = -0.3$, $p > .4$, or $r = -0.5$, $p > .3$, respectively); (b) the total number of $SC123^+$ human cells and the allodynia (supplemental online Table 3) or hyperalgesia measures (Fig. 7C, 7D, Pearson $r = -0.5$, $p > .2$, or $r = -0.2$, $p > .6$,

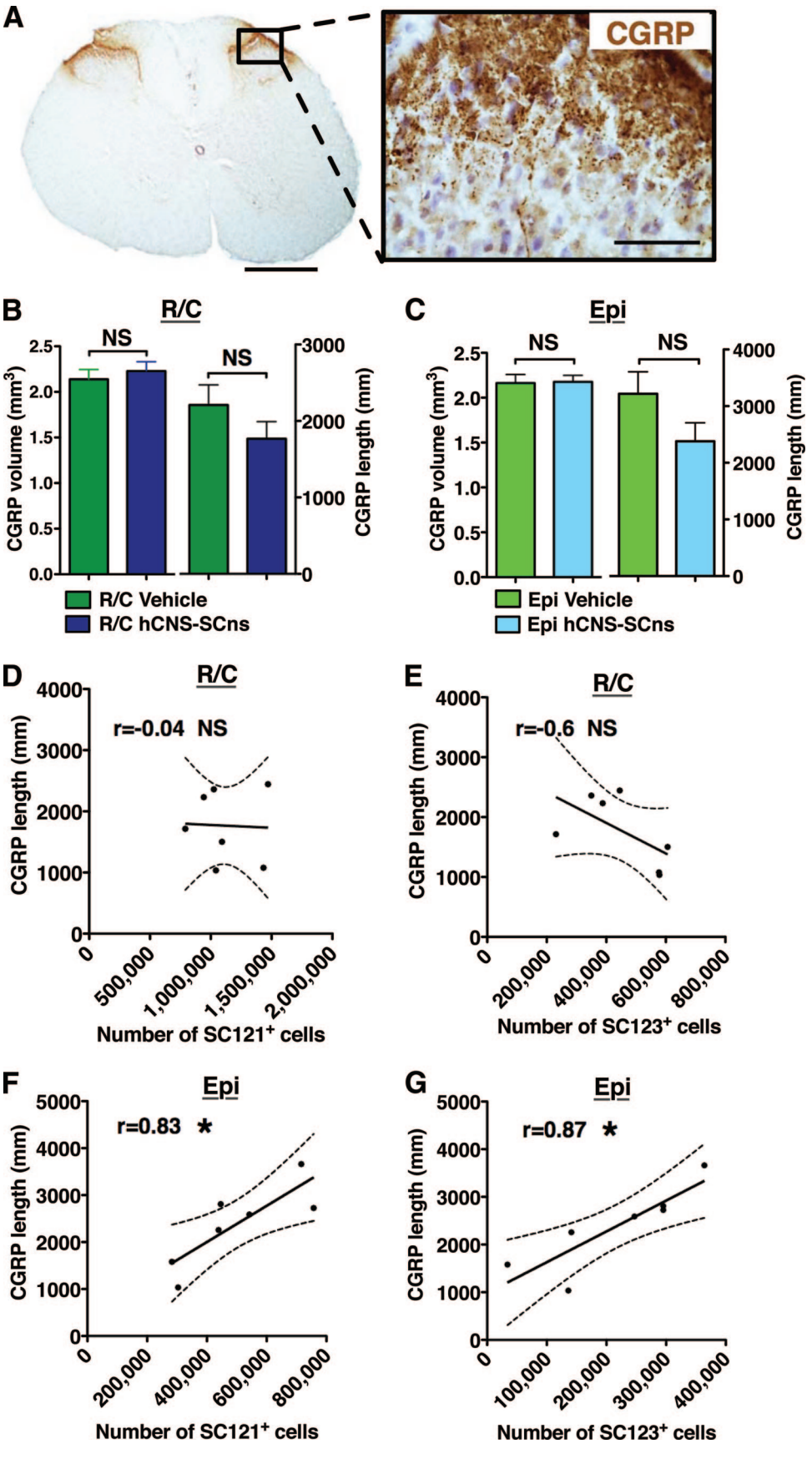
A
CGRP
B
R/C
NS
NS
CGRP volume (mm3)
CGRP length (mm)
R/C Vehicle
R/C hCNS-SCns
C
Epi
NS
NS
CGRP volume (mm3)
CGRP length (mm)
Epi Vehicle
Epi hCNS-SCns
D
R/C
r=-0.04 NS
CGRP length (mm)
Number of SC121+ cells
E
R/C
r=-0.6 NS
CGRP length (mm)
Number of SC123+ cells
F
Epi
r=0.83 *
CGRP length (mm)
Number of SC121+ cells
G
Epi
r=0.87 *
CGRP length (mm)
Number of SC123+ cells

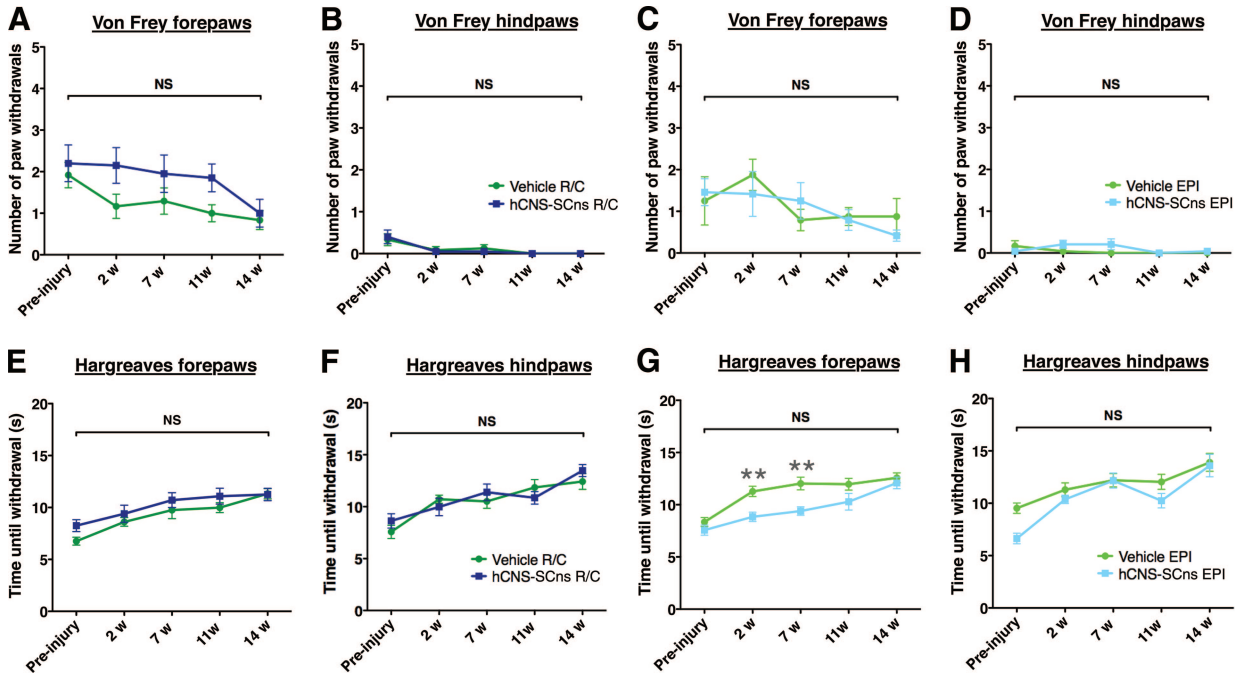

Figure 6. hCNS-SCns transplantation either in intact parenchyma or at injury epicenter at 9 days postinjury does not contribute to development of allodynia or hyperalgesia. All analyses were conducted by repeated-measures two-way analysis of variance. Using the von Frey allodynia test, no significant two-way interaction effects were found between the number of forepaw or hind paw withdrawals in the rostral/caudal (R/C) **(A, B)** or EPI **(C, D)** cohorts over time (black brackets). The R/C transplant cohort did show a significant main effect for the group (R/C vehicle vs. R/C hCNS-SCns) in the number of forepaw withdrawals **(A)** ($p < .03$); however, there were no significant effects for forepaw R/C vehicle versus R/C hCNS-SCns at any individual time point of analysis (Bonferroni post hoc test, $p > .05$). Furthermore, there was no trend for an increase in paw withdrawals over time, and no significant difference between R/C vehicle or hCNS-SCns at 14 weeks post-transplant (wpt) (Student's two-tailed test, $p > .3$) **(A)**. Using the Hargreaves hyperalgesia test, no significant two-way interaction effects were found between forepaw or hind paw withdrawal time in the R/C **(E, F)** or EPI **(G, H)** cohorts over time (black brackets), and no significant differences were observed at any time point of analysis (preinjury or 2, 7, 11, or 14 wpt; Bonferroni post hoc test, $p > .05$). The EPI transplant cohort did show a significant main effect for the group (EPI vehicle vs. EPI hCNS-SCns) in forepaw withdrawal time **(G)** ($p < .003$), and withdrawal time in the EPI transplant cohort was significantly shorter at 2 and 7 wpt (Bonferroni post hoc test, $p < .01$; gray asterisks). However, there was no trend for a decrease in paw withdrawal time over the course of the experiment, and no significant difference was observed between the cohorts at 14 wpt (Student's two-tailed test, $p > .5$). Abbreviations: EPI, epicenter; hCNS-SCns, human central nervous system-derived neural stem cell; NS, not significant; w, weeks.

respectively); (c) the CGRP fiber volume; or (d) the CGRP length and the allodynia or hyperalgesia measures (supplemental online Table 3). These data suggest that neither R/C nor EPI hCNS-SCns transplantation induced progressive or increased sensitivity to mechanical or heat stimuli. Moreover, despite the relationship between $SC121^+$ cells, $SC123^+$ astrocytes and CGRP fiber length in the EPI transplant cohort (Fig. 5), we did not observe increased sensitivity for mechanical or heat stimuli (Fig. 7).

Discussion

Comparison of the effect of subacute hCNS-SCns transplantation either into the injury epicenter or into the intact parenchyma rostral and caudal to the epicenter in an immunodeficient ATN rat SCI model revealed that cells in both paradigms engrafted and migrated away from the injection sites toward parenchyma. Critically, ATN rats in the EPI cohort did not exhibit either restriction of or sustained localization of hCNS-SCns within the cavity. Furthermore, no significant differences in migration distance were observed between EPI and R/C transplant cohorts, suggesting that cells in EPI transplanted animals migrated into adjacent spared tissue either following chemotactic signals in the surrounding spared tissue or in response to repulsive signals within the epicenter. An alternative reason for this observation could be that the transplantation failed to effectively target the cavity, yielding a majority of surviving cells in the adjacent parenchyma.

Figure 5. Relationship of human cell number and astrocytic fate to CGRP fiber sprouting. **(A):** The transplantation site cohorts did not show altered CGRP fiber volume or sprouting in dorsal horn laminae III–IV. Scale bars = 500 and 50 μm. **(B):** CGRP fiber volume and length in the rostral/caudal (R/C) vehicle and transplant cohorts. No significant differences were found between the cohorts (Student's t test; $p > .5$ and $p > .2$, respectively). **(C):** CGRP fiber volume and length in the Epi vehicle and transplant cohorts. No significant differences were found between the cohorts (Student's t test; $p > .9$ and $p > .1$, respectively). Error bars indicate SEM. **(D, E):** In the R/C transplant cohort, Pearson correlation coefficients revealed no correlation between the CGRP fiber length and the estimated total number of $SC121^+$ human cells or the estimated total number of $SC123^+$ astrocytes at 14 weeks post-transplant (wpt) (Pearson $r = -0.04$ and -0.6, respectively, NS, two-tailed t test); $n = 7$ rats. However, a significant positive correlation was found between the CGRP fiber length and the estimated total number of $SC121^+$ human cells **(F)** or the estimated total number of $SC123^+$ astrocytes **(G)** in the Epi transplant cohort at 14 wpt (Pearson $r = 0.83$ and 0.87, respectively; $*$, $p < .05$, two-tailed t test); $n = 7$ rats. x-y scatter plots show individual data points (dots) and the connective curve with $\pm$SEM (dashed lines). Abbreviations: CGRP, calcitonin gene-related peptide; Epi, epicenter; hCNS-SCns, human central nervous system-derived neural stem cell; NS, not significant.

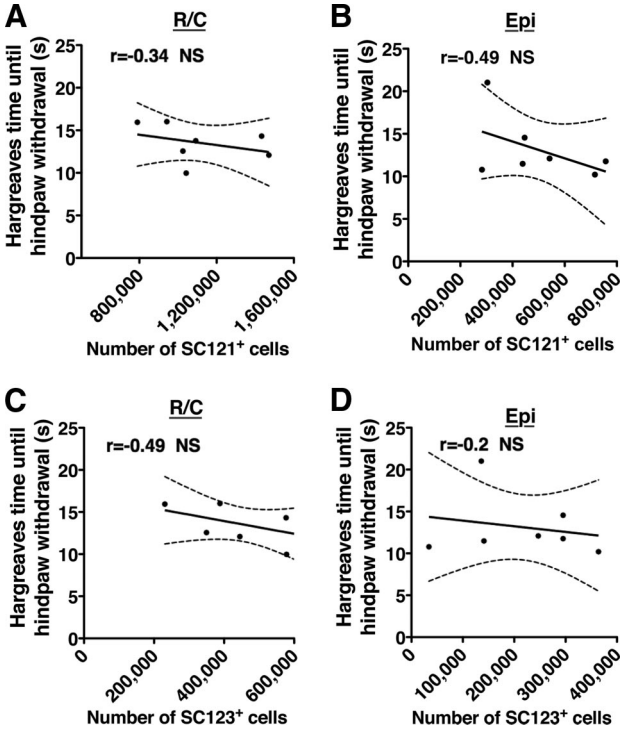

Figure 7. Correlation coefficients revealed no relationship between the Hargreaves paw withdrawal time and the estimated total number of $SC121^+$ human cells in the R/C **(A)** or Epi **(B)** transplant cohort, or the estimated total number of $SC123^+$ astrocytes in the R/C **(C)** or Epi **(D)** transplant cohort at 14 weeks post-transplant. *x-y* scatter plots show individual data points (dots) and connective curve with ±SEM (dashed lines). $n = 7$ mice/cohort, Pearson $r = -0.34$, -0.49, -0.49, and -0.2, respectively, NS, two-tailed *t* test. Abbreviations: Epi, epicenter; NS, not significant; R/C, rostral/caudal.

However, it is unlikely that all animals in the EPI cohort could have received injections into spared tissue rather than cavity, particularly considering the large cavity size in ATN rats, suggesting that this possibility cannot account for these observations. Cell migration away from the injection site can be considered as either a positive or a negative outcome. Our previous studies in NOD-scid mice suggest that both the number of engrafted hCNS-SCns, and the migration of engrafted cells away from the injection sites and into the spared parenchyma distal to the epicenter correlate with behavioral improvement [1–3] (Hooshmand MJ, Nguyen HX, Hong S et al., manuscript in preparation). On the other hand, filling of the spinal cord injury epicenter with either human fetal spinal cord tissue or glial restricted precursors has been suggested to prevent cavity formation and expansion in rodents [37, 38] and humans [39] and/or to form a bridge supporting axon growth [15].

Overall engraftment success in ATN rats was not as high as we have previously achieved in NOD-scid mice, which not only lack T and B cells but also exhibit reduced numbers of natural killer (NK) cells, granulocytes, and macrophages [25, 40]. Additionally, R/C animals exhibited a more than twofold greater number of total human cells surviving at 14 wpt in comparison with EPI animals, suggesting altered survival or engraftment kinetics between the R/C and EPI cohorts. Both human cell engraftment and migration could be affected by intrinsic factors of the transplanted cell population, the initial cell transplant dose, or post-SCI transplantation timing, as well as factors in the inflammatory microenvironment either at the epicenter or in the spared parenchyma. In this regard, some studies have observed retention of transplanted cells at the injury epicenter or migration of transplanted cells toward the injury epicenter [20, 22, 24] (Hooshmand MJ, Nguyen HX, Hong S et al., manuscript in preparation). However, in the present study, the intrinsic factors of the cell population, the initial dose, and transplant timing were all held constant, suggesting that the hCNS-SCns survival or proliferation in the EPI cohort was affected by the microenvironmental factors in the injury epicenter.

The activation of the immune system can influence human neural stem cell engraftment and differentiation [25, 41–43] (Hooshmand MJ, Nguyen HX, Hong S et al., manuscript in preparation). Transplantation in injured or uninjured central nervous system of immunocompetent or insufficiently immunosuppressed models may lead not only to poor engraftment [25, 44] but also to bias toward an astroglial lineage or possibly retention as undifferentiated precursors [20, 22, 24]. Whether transplantation into the primary injury site versus the spared tissue parenchyma can also affect cell fate has not previously been reported. In the present study, the sum of the human cells positive for the three neural lineage specific markers examined was nearly 100% at 14 wpt, indicating that nearly all the human cells had entered the lineage-specific differentiation process regardless of transplantation site. Furthermore, approximately half of engrafted hCNS-SCns in either transplant cohort differentiated toward an oligodendroglial lineage, as previously observed after R/C transplantation in NOD-scid SCI mice [2, 3]. These data suggest that the 9 dpi SCI microenvironment can remain permissive for oligodendrogenesis regardless of the transplant location. However, given the potential role of transplantation timing in cell fate determination [5, 45], it seems likely that a combination of postinjury transplant timing, location, and inflammatory microenvironment, as well as other as yet undefined local cues, contributes to defining hCNS-SCns fate after transplantation.

Interestingly, ATN rats in the both R/C and EPI transplant cohorts demonstrated a relatively higher proportion of human astrocytes (~40%) compared with our previous studies in NOD-scid mice (5%–15%) [2, 3]. In contrast to NOD-scid mice, ATN rats exhibit increased activation of B cells, macrophages, and NK cells [46–49]. We have recently observed that immune cell populations in the transplantation microenvironment can direct cell fate (Hooshmand MJ, Nguyen HX, Hong S et al., manuscript in preparation), suggesting that a parallel mechanism could play a role in directing astroglial differentiation in the ATN rat. Although transplantation site did not alter the overall proportion of hCNS-SCns exhibiting astroglial differentiation, the majority of $SC123^+$ human astrocytes in both cohorts were found rostral to the injury epicenter. This was particularly striking in the EPI transplant cohort, where human astrocytes peaked adjacent to the rostral injury epicenter. In this analysis, positional data were plotted relative to the injury epicenter, which was designated based on identification of the tissue section containing the largest cross-sectional lesion area. However, a majority of ATN rats exhibited large cavities extending into the rostral spinal cord. These data suggest that engrafted human cells may follow the extension of cavitation in the rostral direction or that microenvironmental factors in the parenchyma rostral from the injury epicenter promote astroglial differentiation or are highly chemotactic for human astrocytes and their precursors at the subacute stage of SCI.

Predominant astrogliogenesis and alterations in sprouting of CGRP sensory fibers have been reported to associate with the development of neurological pain in animals receiving neural stem cells transplants after SCI [24, 36]. However, CGRP fiber sprouting is not always associated with behavioral measures of nociception after SCI [50]. In our study, no changes were found in dorsal horn laminae III–IV CGRP volume or fiber length, or in behavioral sensory measures of transplanted versus control animals in the R/C transplant cohort. In parallel, there was no relationship between the number of engrafted human cells and any of these parameters in the R/C cohort. In contrast, although there was no significant overall increase in CGRP fiber volume or sprouting between the EPI vehicle and EPI transplant groups, there was a significant positive correlation between the total number of engrafted human cells (including human astrocytes) and increased CGRP length in the EPI transplant animals. These data suggest that the higher localized density of human astrocytes rostral to the epicenter in the EPI transplant cohort may modulate afferent fiber plasticity. Critically, however, despite this finding, no changes in mechanical allodynia or thermal hyperalgesia measures were observed in the EPI cohort.

Conclusion

hCNS-SCns transplantation in either the injury epicenter or the intact parenchyma at 9 days after moderate contusion injury did not alter human cell engraftment or differentiation or induce mechanical allodynia or thermal hyperalgesia at 14 wpt. Given that the numbers of surviving human cells were significantly greater in the R/C cohort than in the EPI cohort at 14 wpt, these data suggest that transplantation into the intact R/C parenchyma may be preferable to transplantation into the epicenter for this cell population.

Acknowledgments

We thank the staff of the Christopher and Dana Reeve Foundation SCI Core Facility, especially Rebecca Nishi, M.S., and Hongli Liu for their help with animal surgeries. We also thank Kameelah Abdullah, B.S., Kevin Beck, Ph.D., Daniel Cantu, B.S., and Kevin Huang, B.S., for technical assistance. This work was supported by National Institutes of Health/National Institute of Neurological Disorders and Stroke (NIH/NINDS) R01-NS049885 and the Christopher Reeve Foundation AAC-2005 (to A.J.A.), as well as by California Institute for Regenerative Medicine (CIRM) Stem Cell Training Grant T1-00008, the University of California's Alliance for Graduate Education and the Professoriate (UC AGEP) Fellowship NSF HRD0450366 (to D.L.S.), and CIRM Postdoctoral Training Grant TG2-01152 (to K.M.P.).

Author Contributions

K.M.P.: collection and/or assembly of data, data analysis and interpretation, manuscript writing; D.L.S.: collection and/or assembly of data, data analysis; N.U.: provision of study material, data analysis and interpretation; B.J.C.: conception and design, data analysis and interpretation; A.J.A.: conception and design, financial support, data analysis and interpretation, manuscript writing, final approval of manuscript.

Disclosure of Potential Conflicts of Interest

N.U. has compensated employment and stock options from StemCells Inc.

References

1 Salazar D, Uchida N, Hamers F et al. Human neural stem cells differentiate and promote locomotor recovery in an early chronic spinal cord injury NOD-scid mouse model. PLoS One 2010;5:e12272.

2 Cummings BJ, Uchida N, Tamaki SJ et al. Human neural stem cells differentiate and promote locomotor recovery in spinal cord-injured mice. Proc Natl Acad Sci USA 2005;102:14069–14074.

3 Hooshmand MJ, Sontag CJ, Uchida N et al. Analysis of host-mediated repair mechanisms after human CNS-stem cell transplantation for spinal cord injury: Correlation of engraftment with recovery. PLoS One 2009;4:e5871.

4 Tamaki SJ, Jacobs Y, Dohse M et al. Neuroprotection of host cells by human central nervous system stem cells in a mouse model of infantile neuronal ceroid lipofuscinosis. Cell Stem Cell 2009;5:310–319.

5 Uchida N, Chen K, Dohse M et al. Human neural stem cells induce functional myelination in mice with severe dysmyelination. Sci Transl Med 2012;4:155ra136.

6 Uchida N, Buck DW, He D et al. Direct isolation of human central nervous system stem cells. Proc Natl Acad Sci USA 2000;97:14720–14725.

7 Faulkner JR, Herrmann JE, Woo MJ et al. Reactive astrocytes protect tissue and preserve function after spinal cord injury. J Neurosci 2004;24:2143–2155.

8 Rooney GE, Endo T, Ameenuddin S et al. Importance of the vasculature in cyst formation after spinal cord injury. J Neurosurg Spine 2009;11:432–437.

9 Stokes BT, Jakeman LB. Experimental modelling of human spinal cord injury: A model that crosses the species barrier and mimics the spectrum of human cytopathology. Spinal Cord 2002;40:101–109.

10 Fawcett JW. Overcoming inhibition in the damaged spinal cord. J Neurotrauma 2006;23:371–383.

11 Rolls A, Shechter, R, Schwartz M. The bright side of the glial scar in CNS repair. Nat Rev Neurosci 2009;10:235–241.

12 Sun F, Lin C-LG, McTigue D et al. Effects of axon degeneration on oligodendrocyte lineage cells: Dorsal rhizotomy evokes a repair response while axon degeneration rostral to spinal contusion induces both repair and apoptosis. Glia 2010;58:1304–1319.

13 Liu Y, Kim D, Himes B et al. Transplants of fibroblasts genetically modified to express BDNF promote regeneration of adult rat rubrospinal axons and recovery of forelimb function. J Neurosci 1999;19:4370–4387.

14 Keane R, Davis, A, Dietrich W. Inflammatory and apoptotic signaling after spinal cord injury. J Neurotrauma 2006;23:335–344.

15 Davies J, Huang C, Proschel C et al. Astrocytes derived from glial-restricted precursors promote spinal cord repair. J Biol 2006;5:7.

16 Boido M, Garbossa, D, Vercelli A. Early graft of neural precursors in spinal cord compression reduces glial cyst and improves function. J Neurosurg Spine 2011;15:97–106.

17 Marques S, Almeida F, Fernandes A et al. Predifferentiated embryonic stem cells promote functional recovery after spinal cord compressive injury. Brain Res 2010;1349:115–128.

18 Wewetzer K, Radtke C, Kocsis J et al. Species-specific control of cellular proliferation and the impact of large animal models for the use of olfactory ensheathing cells and Schwann cells in spinal cord repair. Exp Neurol 2011;229:80–87.

19 Wright KT, El Masri W, Osman A et al. Concise review: Bone marrow for the treatment of spinal cord injury: Mechanisms and clinical applications. Stem Cells 2011;29:169–178.

20 Chow S, Moul J, Tobias C et al. Characterization and intraspinal grafting of EGF/bFGF-dependent neurospheres derived from embryonic rat spinal cord. Brain Res 2000;874:87–106.

21 Liu S, Qu Y, Stewart T et al. Embryonic stem cells differentiate into oligodendrocytes and myelinate in culture and after spinal cord

transplantation. Proc Natl Acad Sci USA 2000; 97:6126–6131.

22 Cao Q, Zhang Y, Howard R et al. Pluripotent stem cells engrafted into the normal or lesioned adult rat spinal cord are restricted to a glial lineage. Exp Neurol 2001;167:48–58.

23 Hofstetter C, Schwarz E, Hess D et al. Marrow stromal cells form guiding strands in the injured spinal cord and promote recovery. Proc Natl Acad Sci USA 2002;99:2199–2204.

24 Macias M, Syring M, Pizzi M et al. Pain with no gain: Allodynia following neural stem cell transplantation in spinal cord injury. Exp Neurol 2006;201:335–348.

25 Anderson A, Haus D, Hooshmand M et al. Achieving stable human stem cell engraftment and survival in the CNS: Is the future of regenerative medicine immunodeficient? Reg Med 2011;6:367–406.

26 Davies J, Pröschel C, Zhang N et al. Transplanted astrocytes derived from BMP- or CNTF-treated glial-restricted precursors have opposite effects on recovery and allodynia after spinal cord injury. J Biol 2008;7:24.

27 Calmels P, Mick G, Perrouin-Verbe B et al. Neuropathic pain in spinal cord injury: Identification, classification, evaluation. Ann Phys Rehabil Med 2009;52:83–102.

28 Thomas E. A history of haemopoietic cell transplantation. Br J Haematol 1999;105:330–339.

29 Moalem G, Xu K, Yu L. T lymphocytes play a role in neuropathic pain following peripheral nerve injury in rats. Neuroscience 2004;129: 767–777.

30 Hains B, Johnson K, Eaton M et al. Serotonergic neural precursor cell grafts attenuate bilateral hyperexcitability of dorsal horn neurons after spinal hemisection in rat. Neuroscience 2003;116:1097–1110.

31 Hargreaves K, Dubner R, Brown F et al. A new and sensitive method for measuring thermal nociception in cutaneous hyperalgesia. Pain 1988;32:77–88.

32 Horiuchi H, Ogata T, Morino T et al. Adenosine A1 receptor agonists reduce hyperalgesia after spinal cord injury in rats. Spinal Cord 2010;48:685–690.

33 Salazar DL, Uchida N, Hamers FP et al. Human neural stem cells differentiate and promote locomotor recovery in an early chronic spinal cord injury NOD-scid mouse model. PLoS One 2010;5:e12272.

34 Finnerup N, Johannesen I, Sindrup S et al. Pain and dysesthesia in patients with spinal cord injury: A postal survey. Spinal Cord 2001; 39:256–262.

35 Christensen M, Hulsebosch C. Spinal cord injury and anti-NGF treatment results in changes in CGRP density and distribution in the dorsal horn in the rat. Exp Neurol 1997;147: 463–475.

36 Hofstetter C, Holmström N, Lilja J et al. Allodynia limits the usefulness of intraspinal neural stem cell grafts; directed differentiation improves outcome. Nat Neurosci 2005;8:346–353.

37 Giovanini M, Reier P, Eskin T et al. Characteristics of human fetal spinal cord grafts in the adult rat spinal cord: Influences of lesion and grafting conditions. Exp Neurol 1997;148: 523–543.

38 Akesson E, Kjaeldgaard A, Seiger A. Human embryonic spinal cord grafts in adult rat spinal cord cavities: Survival, growth, and interactions with the host. Exp Neurol 1998;149: 262–276.

39 Thompson F, Reier P, Uthman B et al. Neurophysiological assessment of the feasibility and safety of neural tissue transplantation in patients with syringomyelia. J Neurotrauma 2001;18:931–945.

40 Prochazka M, Gaskins HR, Shultz LD et al. The nonobese diabetic scid mouse: Model for spontaneous thymomagenesis associated with immunodeficiency. Proc Natl Acad Sci USA 1992;89:3290–3294.

41 Martino G, Pluchino S, Bonfanti L et al. Brain regeneration in physiology and pathology: The immune signature driving therapeutic plasticity of neural stem cells. Physiol Rev 2011;91:1281–1304.

42 Okano H. Neural stem cells and strategies for the regeneration of the central nervous system. Proc Jpn Acad Ser B Phys Biol Sci 2010; 86:438–450.

43 Magnus T, Rao M. Neural stem cells in inflammatory CNS diseases: Mechanisms and therapy. J Cell Mol Med 2005;9:303–319.

44 Ideguchi M, Shinoyama M, Gomi M et al. Immune or inflammatory response by the host brain suppresses neuronal differentiation of transplanted ES cell-derived neural precursor cells. J Neurosci Res 2008;86:1936–1943.

45 Cummings, BJ, Hooshmand, MJ, Salazar DL et al. Human neural stem cell–mediated repair of the contused spinal cord: Timing the microenvironment. In: Ribak CE, Jones EG, Larriva Sahd JA, eds. From Development to Degeneration and Regeneration of the Nervous System. New York, NY: Oxford University Press, 2008:297–322.

46 Rolstad B. The athymic nude rat: An animal experimental model to reveal novel aspects of innate immune responses? Immunol Rev 2001;184:136–144.

47 Vos J, Kreeftenberg J, Kruijt B et al. The athymic nude rat. Immunological characteristics. Clin Immunol Immunopathol 1980;15: 229–2376.

48 Hougen H. The athymic nude rat: Immunobiological characteristics with special reference to establishment of non-antigen-specific t-cell reactivity and induction of antigen-specific. APMIS Suppl 1991;21:1–39.

49 Xia G, Ji P, Rutgeerts O et al. Natural killer cell- and macrophage mediated discordant guinea pig–>rat xenograft rejection in the absence of complement, xenoantibody and T cell immunity. Transplantation 2000;70:86–93.

50 Barritt A, Davies M, Marchand F et al. Chondroitinase ABC promotes sprouting of intact and injured spinal systems after spinal cord injury. J Neurosci 2006;26:10856–10867.

See www.StemCellsTM.com for supporting information available online.